Optically Measured Power Balances of Anomalous Discharges of Mixtures of Argon, Hydrogen, and Potassium, Rubidium, Cesium, or Strontium Vapor

Randell L. Mills
Nelson Greenig
Steven Hicks
BlackLight Power, Inc.
493 Old Trenton Road
Cranbury, NJ 08512

The power balances of gas cells having atomized hydrogen from pure hydrogen alone, an argon-hydrogen mixture alone, or pure hydrogen or an argon-hydrogen mixture with vaporized potassium, rubidium, cesium, strontium, sodium, or magnesium were measured by integrating the total light output corrected for spectrometer system response and energy over the visible range as the input power was varied. The light emitted for power supplied to the glow discharge increased by over two orders of magnitude depending on the presence of less than 1% partial pressure of certain of the alkali or alkaline earth metals in hydrogen gas or argon-hydrogen gas mixtures. Whereas, other chemically similar metals had no effect on the plasma. The metal vapor enhancement of the emission was dramatically greater with an argon-hydrogen mixture versus pure hydrogen, and a 97% argon and 3% hydrogen mixture had greater emission than either gas alone. Only those atoms or ions which ionize at integer multiples of the potential energy of atomic hydrogen, potassium, cesium, Rb^+, strontium, and Ar^+ caused an anomalous increase in emission; whereas, no anomalous behavior was observed in the case of $Mg(m)$ and $Na(m)$ which do not provide a reaction with a net enthalpy of a multiple of the potential energy of atomic hydrogen. The light intensity versus power input of a mixture of these metals with hydrogen, argon, or argon-hydrogen gas was the same as that of the corresponding gas alone. At an input power to the glow discharge of 10 watts, the optically measured light output power of a mixture of strontium, cesium, potassium, or rubidium with 97% argon and 3% hydrogen was 750, 70, 16, and 13 $\mu W/cm^2$, respectively. Whereas, the optically measured light output power of the argon-hydrogen mixture (97/3%) alone or with sodium or magnesium was about 11 $\mu W/cm^2$, and the result for hydrogen or argon alone was 1.5 $\mu W/cm^2$. A temperature dependence of some of the anomalous plasmas was determined corresponding to the metal's partial pressure dependence on temperature. These studies provide useful parameters for the optimization of the catalytic reaction of atomic hydrogen.

I. INTRODUCTION

Based on the solution of a Schrödinger-type wave equation with a nonradiative boundary condition based on Maxwell's equations, Mills [1-31] predicts that atomic hydrogen may undergo a catalytic reaction with certain atomized elements or certain gaseous ions which singly or multiply ionize at integer multiples of the potential energy of atomic hydrogen, $27.2\,eV$. For example, cesium atoms ionize at an integer multiple of the potential energy of atomic hydrogen, $m \cdot 27.2\,eV$. The enthalpy of ionization of Cs to Cs^{2+} has a net enthalpy of reaction of $27.05135\,eV$, which is equivalent to $m=1$ [32]. And, the reaction Ar^{+} to Ar^{2+} has a net enthalpy of reaction of $27.63\,eV$, which is equivalent to $m=1$ [32]. In each case, the reaction involves a nonradiative energy transfer to form a hydrogen atom that is lower in energy than unreacted atomic hydrogen. The product hydrogen atom has an energy state that corresponds to a fractional principal quantum number. Recent analysis of mobility and spectroscopy data of individual electrons in liquid helium show direct experimental confirmation that electrons may have fractional principal quantum energy levels [33]. The lower-energy hydrogen atom is a highly reactive intermediate which further reacts to form a novel hydride ion. Emission was observed previously from a continuum state of Cs^{2+} and Ar^{2+} at $53.3\,nm$ and $45.6\,nm$, respectively [2]. The single emission feature with the absence of the other corresponding Rydberg series of lines from these species confirmed the resonate nonradiative energy transfer of $27.2\,eV$ from atomic hydrogen to atomic cesium or Ar^{+}. The catalysis product, a lower-energy hydrogen atom, was predicted to be a highly reactive intermediate which further reacts to form a novel hydride ion. The predicted hydride ion of hydrogen catalysis by either cesium atom or Ar^{+} catalyst is the hydride ion $H^{-}(1/2)$. This ion was observed spectroscopically at $407\,nm$ corresponding to its predicted binding energy of $3.05\,eV$. The catalytic reaction with the formation the hydride ions are given in the Appendix.

Typically the emission of extreme ultraviolet light from hydrogen gas is achieved via a discharge at high voltage, a high power inductively coupled plasma, or a plasma created and heated to extreme temperatures by RF coupling (e.g. $>10^{6}\,K$) with confinement provided by a toroidal

magnetic field. Observation of intense extreme ultraviolet (EUV) emission at low temperatures (e.g. $\approx 10^3\ K$) from atomic hydrogen and certain atomized elements or certain gaseous ions [2-16] has been reported previously. The only pure elements that were observed to emit EUV were those wherein the ionization of t electrons from an atom to a continuum energy level is such that the sum of the ionization energies of the t electrons is approximately $m \cdot 27.2\ eV$ where t and m are each an integer. Potassium, cesium, and strontium atoms and Rb^+ ion ionize at integer multiples of the potential energy of atomic hydrogen and caused emission. Whereas, the chemically similar atoms, sodium, magnesium and barium, do not ionize at integer multiples of the potential energy of atomic hydrogen and caused no emission.

Additional prior studies that support the possibility of a novel reaction of atomic hydrogen which produces an anomalous discharge and produces novel hydride compounds include extreme ultraviolet (EUV) spectroscopy [2-6, 9-16], plasma formation [2-16], power generation [3-4, 9, 31], and analysis of chemical compounds [17-31].

1.) Lines observed at the Institut Fur Niedertemperatur-Plasmaphysik e.V. by EUV spectroscopy could be assigned to transitions of atomic hydrogen to lower energy levels corresponding to lower energy hydrogen atoms and the emission from the excitation of the corresponding hydride ions [6]. For example, the product of the catalysis of atomic hydrogen with potassium metal, $H\left[\frac{a_H}{4}\right]$ may serve as both a catalyst and a reactant to form $H\left[\frac{a_H}{3}\right]$ and $H\left[\frac{a_H}{6}\right]$. The transition of $H\left[\frac{a_H}{4}\right]$ to $H\left[\frac{a_H}{6}\right]$ induced by a multipole resonance transfer of $54.4\ eV$ $(2 \cdot 27.2\ eV)$ and a transfer of $40.8\ eV$ with a resonance state of $H\left[\frac{a_H}{3}\right]$ excited in $H\left[\frac{a_H}{4}\right]$ is represented by

$$H\left[\frac{a_H}{4}\right] + H\left[\frac{a_H}{4}\right] \rightarrow H\left[\frac{a_H}{6}\right] + H\left[\frac{a_H}{3}\right] + 176.8\ eV \qquad (1)$$

The predicted $176.8\ eV$ (70.2 Å) photon is a close match with the observed 73.0 Å line. The energy of this line emission corresponds to an

equivalent temperature of 1,000,000 °C and an energy over 100 times the energy of combustion of hydrogen.

2.) Transitions of atomic hydrogen to lower energy levels corresponding to lower energy hydrogen atoms has been identified in the extreme ultraviolet emission spectrum from interstellar medium [34].

3.) An anomalous plasma with hydrogen-potassium mixtures has been reported in an experiment similar to the present plasma experiments [7-8, 10]. In experiments performed at the Institut Fur Niedertemperatur-Plasmaphysik e.V., an anomalous plasma formed with hydrogen-potassium mixtures wherein the plasma decayed with a two second half-life which was the thermal decay time of the filament which dissociated molecular hydrogen to atomic hydrogen when the electric field was set to zero [7, 10]. This experiment showed that hydrogen line emission was occurring even though the voltage between the heater wires was set to and measured to be zero and indicated that the emission was due to a reaction of potassium atoms with atomic hydrogen which confirms a new chemical source of power. Potassium atoms ionize at an integer multiple of the potential energy of atomic hydrogen, $m \cdot 27.2\,eV$. The enthalpy of ionization of K to K^{3+} has a net enthalpy of reaction of $81.7426\,eV$, which is equivalent to $m = 3$.

4.) An anomalous plasma of hydrogen and certain alkali ions formed at low temperatures (e.g. $\approx 10^3\,K$) as recorded via EUV spectroscopy and the hydrogen Balmer and alkali line emissions in the visible range. The observed plasma formed at low temperatures (e.g. $\approx 10^3\,K$) from atomic hydrogen generated at a tungsten filament that heated a titanium dissociator and a catalyst comprising one of potassium, rubidium, cesium, and their carbonates and nitrates. These atoms and ions ionize to provide a catalyst with a net enthalpy of reaction of an integer multiple of the potential energy of atomic hydrogen ($m \cdot 27.2\,eV$, $m = integer$) to within 0.17 eV and comprise only a single ionization in the case of a potassium or rubidium ion. Whereas, the chemically similar atoms of sodium and sodium and lithium carbonates and nitrates which do not ionize with these constraints caused no emission. To test the electric dependence of the emission, a weak electric field of about 1 V/cm was set and measured to be zero in $< 0.5\,X\,10^{-6}$ sec. An anomalous afterglow duration of about one to two seconds was

recorded in the case of potassium, rubidium, cesium, K_2CO_3, $RbNO_3$, and $CsNO_3$. Hydrogen line or alkali line emission was occurring even though the voltage between the heater wires was set to and measured to be zero. These atoms and ions ionize to provide a catalyst with a net enthalpy of reaction of an integer multiple of the potential energy of atomic hydrogen to within less than the thermal energies at $\approx 10^3\,K$ and comprise only a single ionization in the case of a potassium or rubidium ion. Since the thermal decay time of the filament for dissociation of molecular hydrogen to atomic hydrogen was similar to the anomalous plasma afterglow duration, the emission was determined to be due to a reaction of atomic hydrogen with a catalyst that did not require the presence of an electric field to be functional.

5.) An energetic plasma in hydrogen was generated using strontium atoms as the catalyst. The plasma formed at 1% of the theoretical (Townsend theory) or prior known voltage requirement with 4,000-7,000 times less power input power compared to noncatalyst controls, sodium, magnesium, or barium atoms, wherein the plasma reaction was controlled with a weak electric field [4, 9]. The light output for power input increased to 8600 times that of the control when argon was added to the hydrogen strontium plasma [3].

In the present study, the alkali and alkaline earth metal catalysts and argon ion catalyst which were previously reported to produce anomalous discharges [2-16] were studied with controls to determine their relative performance. Anomalous and normal discharges were observed by visible emission. The anomalous power balances of gas cells were measured by integrating the total light output corrected for spectrometer system response and energy over the visible range as the input power was varied. The measurements were performed on hydrogen, argon, or argon-hydrogen mixtures alone and with vaporized alkali and alkaline earth metals in a stainless steel glow discharge cell. The cathode of the discharge cell was a central tungsten filament. The anode was a cylindrical nickel mesh. A radial electric field existed between the cathode and anode. Power was applied to the electrode to achieve a bright plasma which was recorded over the wavelength range $350 \le \lambda \le 750\,nm$. In addition, the optimum argon to hydrogen ratio for producing the maximum anomalous emission with potassium was

determined. Some of the anomalous plasmas were further studied for temperature dependence corresponding to the catalyst metal's partial pressure dependence on temperature.

II. EXPERIMENTAL

A. Power cell apparatus and procedure

Plasma studies with 1.) hydrogen, argon, argon-hydrogen mixture (97/3%), and argon-hydrogen mixture (90/10%), 2.) sodium, magnesium, cesium, potassium, rubidium, and strontium with hydrogen, 3.) sodium, magnesium, cesium, potassium, rubidium, and strontium with argon, 4.) sodium, magnesium, cesium, potassium, rubidium, and strontium with argon-hydrogen mixture (97/3%), and 5.) potassium with argon-hydrogen mixture (90/10%) were carried out in the cylindrical stainless steel gas cell shown in Figure 1. All experiments were conducted at 650 °C except for studies on the temperature dependence of the light emission versus input power performed on cesium with argon-hydrogen mixture (97/3%), and rubidium with argon-hydrogen mixture (97/3%).

The experimental setup for generating a glow discharge hydrogen plasma and for optically measuring the power balance is shown in Figures 1 and 2. The 304-stainless steel cell was in the form of a tube having an internal cavity of 35.9 cm in length and 7.4 cm in diameter. The top end of the cell was welded to a high vacuum 11.75 cm diameter conflat flange. A silver plated copper gasket was placed between a mating flange and the cell flange. The two flanges were held together with 10 circumferential bolts. The mating flange contained five penetrations comprising 1&2.) two stainless steel thermocouple wells which placed thermocouples in the cell interior 2 cm from the discharge gap and 2 cm from the cell axis, 3.) a 1 cm diameter stainless steel light path tube located 2 cm off-axis that passed through the flange, extended 10 cm into the cell to a location 1 cm from a discharge volume between two electrodes, and had a saphire window view port at the interior tube end, 4.) a 1 cm stainless steel catalyst delivery tube welded flush with the flange top, and 5.) a stainless steel tube (1 cm diameter and 100 cm in length) welded flush with the bottom surface of the top flange that

served as a vacuum line from the cell and contained a center coaxial assembly that extended 35 cm into the cell. The assembly comprised a 0.15 cm ID stainless steel hydrogen or argon-hydrogen supply tube, anode power connection, and electrode assembly support surrounded by a high density Alumina tube electrical insulator (0.4 cm ID and 0.7 OD).

The glow discharge electrode assembly shown in Figure 1 comprised an axial inner tungsten spiral wire (1.9 mm OD by 200 cm long) anode (2.1 cm by 10 cm long) and a circumferential nickel mesh cathode (60 cm ID by 20 cm long, Belleville Wire Cloth Co., Inc.) supported by an Alumina frame comprising a top and bottom Alumina disc (6 cm OD Alpha Aesar 3318). The Alumina tube electrical insulator of the coaxial assembly stopped at the bottom Alumina disc. A second spirally grooved Alumina tube (2.1 cm OD by 10 cm long Alpha Aesar 33204) was concentric to the insulator and supported the tungsten anode which terminated at the top without a connection. The bottom of the tungsten wire anode passed through a hole in the Alumina tube electrical insulator and a hole in the bottom Alumina disc to connect with the anode power connection. The connection was made by compressing the tungsten wire between two collar clamps wherein the top clamp also served to connect the electrode assembly to the electrode assembly support. The cathode was connected to the top flange by a stainless steel wire.

Concentrated aqueous solutions ($\approx 0.6\,M$) of sodium carbonate (Alfa Aesar ACS grade 99+ %), potassium carbonate (Alfa Aesar ACS grade 99+ %), rubidium carbonate (Alfa Aesar 99 %), cesium carbonate (Alfa Aesar 99 %), and magnesium carbonate (Alfa Aesar Puratronic grade 99.996 %) were sprayed onto the nickel mesh cathode and dried with a hot air gun. The application of the metal carbonate was carried out until the surface was completely covered with an inorganic film. The electrode assembly comprising the cathode and central anode was placed in the cell as shown in Figure 2. The cell was evacuated through the outer vacuum line with a high vacuum molecular drag pump (Hovac DRI-2) to reach 50 mtorr measured by a 100 torr pressure gauge (MKS Baratron). The vacuum pump valve was then closed. The cell was surrounded by a temperature controlled oven ($\pm 0.3\,°C$ at 650 °C) as shown in Figure 2 having high temperature insulation (AL 30 Zircar), a controller (Omega) type 76000),

and a regulated power supply. Type K thermocouples (Omega) housed in the two stainless steel wells read the cell temperature. The cell was heated and maintained at a temperature of 650 °C except for studies on the temperature dependence of the light emission versus input power. The cell was then pressurized with hydrogen (99.999% purity) to approximately 100 torr that was flowed through the inner supply tube. The pressure in the supply tube was measured by a 100 torr pressure gauge (MKS Baratron). The cell was then subsequently evacuated through the outer vacuum line to purge CO_2 and gaseous contaminants from the system. The decomposition of the metal carbonate to the corresponding metal was repeated until no further CO_2 was observed with a visible spectrometer (Ocean Optics S2000).

Strontium (Aldrich Chemical Company 99.9 %) metal was supplied to the cell using a transfer apparatus to avoid exposure of the metal to air. The transfer apparatus comprised a reservoir and a ball valve (Swagelok SS-45S8). The strontium was loaded into the reservoir in a glove box under a dry argon atmosphere through the valve passage. The valve was then closed. The transfer assembly was then attached to the catalyst delivery tube. The cell was evacuated through the outer vacuum line to reach 50 mtorr. The vacuum pump valve was then closed. The cell was heated and maintained at a temperature of 300 °C. The strontium was loaded into the cell through the ball valve. The cell was then pressurized with hydrogen (99.999% purity) to approximately 100 torr that was flowed through the inner supply tube. The cell was then subsequently evacuated through the outer vacuum line to purge gaseous contaminants from the system. The cell was heated and maintained at a temperature of 650 °C.

After the metal was formed or loaded into the cell, the cell was operated under gas flow conditions while maintaining a constant gas pressure in the cell with a mass flow controller where the pressure in the hydrogen and argon supply tube outside the furnace was monitored by the 100 torr MKS Baratron absolute pressure gauge. Except where indicated, the gas was ultrahigh purity hydrogen, argon-hydrogen mixture (97/3%), or an argon-hydrogen mixture (90/10%). The gas pressure inside the cell was maintained at about 300 mtorr with a hydrogen flow rate of 5.5 sccm, an argon-hydrogen mixture (97/3%) flow

rate of 5.5 sccm, or an argon flow rate of 5.0 sccm and a hydrogen flow rate of 0.6 sccm, respectively. Each gas flow was controlled by a 20 sccm range mass flow controller (MKS 1179A21CS1BB) with a readout (MKS type 247C). The partial pressure of the metal was determined by its equilibrium vapor pressure at the operating temperature of the cell as given in Table 1.

The field voltage was increased until breakdown occurred. This was confirmed by the spectrometer response to visible light emitted from the cell. The discharge was started and maintained by a DC electric field in the 1.9 cm annular gap between an axial anode and a cylindrical circumferential cathode. The glow discharge power was 0.300 A constant current provided by a custom built (BlackLight Power, Inc.) constant current controller with a response time of $< 0.5 X 10^{-6}$ sec. The quick response time assured the maintenance of a stable plasma as determined by using an oscilloscope to monitor the DC voltage and current. With the current fixed, the power was given by the constant current times the driving voltage. The power was increased by ramping the voltage at constant current and the optical power output was recorded.

B. Optical measurements

A glow discharge was produced in a stainless steel gas cell shown in Figure 2 comprising the axial inner tungsten wire anode and the circumferential nickel mesh cathode shown in Figure 1. An essentially uniform radial electric field existed between the anode and cathode. A 1.6 mm thick UV-grade sapphire window with a 1 cm view diameter provided a visible light path from inside the cell. The viewing direction was parallel to the cell axis. The 1 cm diameter stainless steel light path tube passed through the furnace wall to provide an optical light path from the sapphire window to the furnace exterior. An 0.63 cm diameter quartz rod channeled the light from the window through the light path tube to a collimating lens which was focused on a 100 μm optical fiber located outside the furnace. Spectral data was recorded with a visible spectrometer (Ocean Optics S2000) and stored by a personal computer. To correct for the nonuniform response of the spectrometer system as a function of wavelength and the dependence of energy on wavelength, the

system was calibrated against a reference light source (Ocean Optics LS-1-CAL). A spectral calibration factor was applied to the count rate data at each wavelength to yield the irradiation of the detector in units of energy/time/area/wavelength. The total visible radiant flux incident on the detector was calculated by integrating the spectral irradiation between 400 and 700 nm.

III. RESULTS

A. Comparison of catalysts by optically measured power balance

The optically measured light output power was determined by integrating the total light output corrected for spectrometer system response and energy over the visible range, $350 \leq \lambda \leq 750\,nm$ as the input power was varied. Comparison of hydrogen, argon, and various mixtures of hydrogen and argon with catalysts and noncatalyst controls are given in Figures 3-7 which plot the output light intensity versus power input to the glow discharge. Since the current remained constant at 0.300 A, the voltage can be determined from the power in these figures by multiplying by 3. In Figures 3-5, the results of the test gas alone, sodium or magnesium with hydrogen, and potassium, rubidium, cesium, strontium, sodium, or magnesium with argon are plotted together for convenience since no difference was observed with the metal present. In the case that a plasma could not be achieved at low power, the curve at higher input power was fitted (dotted line) and extended to the lower input power region.

The comparison of the light output power ($\mu W/cm^2$) of 1.) hydrogen, argon, argon-hydrogen mixture (97/3%), and argon-hydrogen mixture (90/10%), 2.) sodium, magnesium, and potassium with hydrogen, 3.) sodium, magnesium, cesium, potassium, rubidium, and strontium with argon, 4.) sodium, magnesium, cesium, potassium, rubidium, and strontium with argon-hydrogen mixture (97/3%), and 5.) potassium with argon-hydrogen mixture (90/10%) is shown in Figures 3-5. The $0\text{-}50\,\mu W/cm^2$ range is shown in Figure 3. At an input power to the glow discharge of 10 watts, the optically measured light output power of both

of a mixture of cesium and argon-hydrogen (97/3%) and a mixture of strontium and argon-hydrogen (97/3%) were off-scale, and the optically measured light output power of a mixture of potassium and argon-hydrogen (90/10%), potassium and argon-hydrogen (97/3%), rubidium and argon-hydrogen (97/3%), argon-hydrogen (97/3%), argon-hydrogen (90/10%), and potassium and hydrogen was 27, 16, 13, 11, 10, and 5 $\mu W/cm^2$, respectively. Whereas, the optically measured light output power of hydrogen or argon alone was 1.5 $\mu W/cm^2$. Thus, at 10 watts, the optically measured light output power trend for these on-scale mixtures was K + Ar + H_2 (90/10%) > K + Ar + H_2 (97/3%) > Rb + Ar + H_2 (97/3%) > Ar + H_2 (97/3%) > Ar + H_2 (90/10%) > K + H_2 > H_2 alone = Na + H_2, Mg + H_2, Ar alone, Na + Ar, Mg + Ar, K + Ar, Rb + Ar, Cs + Ar, Sr + Ar. Magnesium and sodium had no effect on the hydrogen plasma, and no metal had an effect on the argon plasma. For potassium which significantly increased the light output of an argon-hydrogen mixture, the ratio of argon to hydrogen was varied, and the ratio which maximized the optical output power in the visible was determined to be about 90 % argon and 10% hydrogen. Strontium and hydrogen produced a bright plasma which was comparable to the plasma formed with cesium and argon-hydrogen (97%/3%), but was not as stable. Cesium and hydrogen also formed a bright plasma with hydrogen that was less intense and stable then in the case of the plasma formed with argon present. Rubidium and hydrogen showed slightly weaker anomalous emission than potassium and hydrogen.

The comparison of the optically measured light output powers in the range the 0-200 $\mu W/cm^2$ and 0-800 $\mu W/cm^2$ are shown in Figures 4 and 5, respectively. In Figure 4, at an input power to the glow discharge of 10 watts, the optically measured light output power of a mixture of strontium and argon-hydrogen (97/3%) was off-scale. From Figure 5, the optically measured light output power of a mixture of strontium or cesium with 97 % argon and 3 % hydrogen was 750 and 70 $\mu W/cm^2$, respectively. Thus, from the combined results shown in Figures 3-5, the optically measured light output power trend at 10 watts was Sr + Ar + H_2 (97/3%) >> Cs + Ar + H_2 (97/3%) > K + Ar + H_2 (90/10%) > K + Ar + H_2 (97/3%) > Rb + Ar + H_2 (97/3%) > Ar + H_2 (97/3%) > Ar + H_2 (90/10%) > K + H_2 > H_2 alone = Na + H_2, Mg + H_2, Ar alone, Na + Ar, Mg + Ar, K + Ar, Rb +

Ar, Cs + Ar, Sr + Ar. With the addition of strontium to argon-hydrogen (97/3%), the light output was about 75 times higher compared to argon-hydrogen alone and about 500 times higher compared to hydrogen or argon alone.

B. Temperature dependence of catalysts by optically measured power balance

The temperature dependence of the light emission of cesium-argon-hydrogen mixture (97/3%) as a function of input power was studied and compared with the emission of potassium and rubidium with argon-hydrogen mixture (97/3%) at a cell temperature of 650 °C. The comparison of the light output power ($\mu W/cm^2$) of 1.) potassium and argon-hydrogen mixture (97/3%) at a cell temperature of 650 °C, 2.) rubidium and argon-hydrogen mixture (97/3%) at a cell temperature of 650 °C, and 3.) cesium and argon-hydrogen mixture (97/3%) at a cell temperature of 480 °C, 500 °C, 520 °C, 540 °C, 565 °C, and 600 °C is shown in Figure 6. The input power to the glow discharge to achieve an optically measured light output power of $30\,mW/cm^2$ from a mixture of cesium and argon-hydrogen (97/3%) at 480 °C, 500 °C, 520 °C, 540 °C, 565 °C, and 600 °C was 2, 3, 4, 5, 7, and 18 W, respectively. In comparison, the input power to the glow discharge to achieve an optically measured light output power of $30\,mW/cm^2$ from a mixture of potassium or rubidium with argon-hydrogen mixture (97/3%) at 650 °C was 15 and about 33 W, respectively. The optically measured trend of the temperature dependence of the cesium light output power was in order of decreasing temperature. The light output for cesium at the lowest temperature of 480 °C was the greatest at the lowest input powers, but the output was asymptotic at about 4 W input. The cause may be due to a shortage of cesium metal catalyst from the decomposition reaction of the source, Cs_2CO_3. The light output for cesium at the highest temperature of 600 °C was distinguishably lower than the emission for any other temperature. The cause may be due to an excessive cesium vapor pressure which decreased the catalysis rate and excessively increased the conductivity of the plasma.

The data indicates that the catalysis reaction is sensitive to the

cesium vapor pressure with a decrease in rate due to excess cesium vapor pressure. The vapor pressure of cesium as a function of temperature is given in Table 1.

The comparison of the light output power ($\mu W/cm^2$) of 1.) cesium and argon-hydrogen mixture (97/3%) at a cell temperature of 565 °C, and 2.) rubidium and argon-hydrogen mixture (97/3%) at a cell temperature of 470 °C, 500 °C, 535 °C, 560 °C, 600 °C, 620 °C, and 650 °C is shown in Figure 7. The light output for rubidium at the lowest temperature of 470 °C was distinguishably lower than the emission for any other temperature. The cause may be due to a shortage of metal from the decomposition reaction of the source, Rb_2CO_3. The outputs for the cases at the higher temperatures, 560 °C, 600 °C, 620 °C, and 650 °C are very similar in magnitude and behavior showing essentially linear output with input.

The cesium and argon-hydrogen mixture (97/3%) at 565 °C produced the highest output for input at about 7 watt at which point the emission becomes essentially linear with input power. An asymptotic behavior was observed to a lesser extent for rubidium for the intermediate the temperatures, 500 °C and 535 °C. Rubidium at a cell temperature of 500 °C produced the highest output for an input power less that 10 watts. But, the highest difference of about 70 % more emission relative to other cell temperatures was observed from the 535 °C cell which showed a peak emission at 12 W input.

The data indicates that the catalysis reaction is sensitive to the rubidium vapor pressure with a decrease in rate due deviation from an optimum. The vapor pressure of rubidium as a function of temperature is given in Table 1. At 10 watts input, cesium produced about 6 times the output of rubidium at any temperature. This indicates that the reaction is much more dependent on the activity of the particular catalyst then on temperature within a reasonably broad temperature range.

IV. DISCUSSION

The optical power balances of gas cells having atomized hydrogen from an argon-hydrogen mixture alone or pure hydrogen or an argon-hydrogen mixture with vaporized potassium, rubidium as a source of Rb^+

in the glow discharge, cesium, or strontium were measured by integrating the total light output corrected for spectrometer system response and energy over the visible range as the input power was varied. Control experiments were identical except that the pure gas was run alone, or sodium or magnesium replaced the metal catalyst in the case of a metal mixture with hydrogen gas or an argon-hydrogen mixture. The light emitted for power supplied to the glow discharge increased by over two orders of magnitude depending on the presence of less than 1% partial pressure of certain of the alkali or alkaline earth metals in hydrogen gas or argon-hydrogen gas mixtures. Whereas, other chemically similar metals had no effect on the plasma. The metal vapor enhancement of the emission was dramatically greater with an argon-hydrogen mixture versus pure hydrogen, and a 97 % argon and 3 % hydrogen mixture had greater emission than either gas alone. Only those atoms or ions which ionize at integer multiples of the potential energy of atomic hydrogen, potassium, cesium, Rb^+, strontium, and Ar^+ caused an anomalous increase in emission; whereas, no anomalous behavior was observed in the case of $Mg(m)$ and $Na(m)$ which do not provide a reaction with a net enthalpy of a multiple of the potential energy of atomic hydrogen. The light intensity versus power input with these metals were the same as that of the hydrogen gas or argon-hydrogen gas mixture alone.

At an input power to the glow discharge of 10 watts, the optically measured light output power of a mixture of strontium, cesium, potassium, or rubidium with 97 % argon and 3 % hydrogen was 750, 70, 16, and 13 $\mu W/cm^2$, respectively. The emission from potassium with argon-hydrogen mixtures was maximized at a ratio of 90% argon and 10% hydrogen that output 27 $\mu W/cm^2$ of light with 10 W input. The optically measured light output power of the argon-hydrogen mixture (97/3%) and (90/10%) was 11 $\mu W/cm^2$ and 10 $\mu W/cm^2$, respectively. Whereas, the optically measured light output power of a mixture of potassium with hydrogen was 5 $\mu W/cm^2$, and the result for hydrogen or argon alone was 1.5 $\mu W/cm^2$. Thus, at 10 watts, the optically measured light output power trend was Sr + Ar + H_2 (97/3%) >> Cs + Ar + H_2 (97/3%) > K + Ar + H_2 (90/10%) > K + Ar + H_2 (97/3%) > Rb + Ar + H_2 (97/3%) > Ar + H_2 (97/3%) > Ar + H_2 (90/10%) > K + H_2 > H_2 alone = Na + H_2, Mg + H_2, Ar alone, Na + Ar, Mg + Ar, K + Ar, Rb + Ar, Cs + Ar, Sr + Ar. Magnesium and sodium had no

effect on the hydrogen or argon-hydrogen plasma; whereas, addition of potassium to hydrogen or an argon-hydrogen mixture increased the optical output power. At 10 watts input, the addition of argon to the potassium-hydrogen mixture to provide Ar^+ catalyst increased the output by a factor of 3 and 6 for an argon-hydrogen mixture of 97/3% and 90/10%, respectively. The data indicate that the combination of potassium and argon catalyst is not simply additive. This implies that potassium catalyst may increase the amount of Ar^+ catalyst to enhance the catalysis of hydrogen. With the addition of strontium to argon-hydrogen (97/3%), the light output was about 75 times higher compared to argon-hydrogen alone and about 500 times higher compared to hydrogen or argon alone. Thus, strontium catalyst may increase the amount of Ar^+ catalyst to a greater extent than potassium to enhance the catalysis of hydrogen.

Compared to the output of 200 $\mu W/cm^2$ with 10 watts input to the strontium-argon-hydrogen mixture, the power to achieve the same optically measured light output power from the hydrogen controls was estimated to be at a factor of 1000 times greater based on the slope of the light output versus power input plots. The projected kilowatts of input power was not achievable with the experimental apparatus. The results indicate that an extraordinary anomalous plasma formed with a strontium-argon-hydrogen mixture.

A temperature dependence of some of the anomalous plasmas was determined corresponding to the metal's partial pressure dependence on temperature. The optically measured trend of the temperature dependence of the cesium light output power was in order of decreasing temperature. The optimum operating temperature for cesium-argon-hydrogen over the range 480 °C - 600 °C was determined to be 480 °C. The light output for cesium at the highest temperature of 600 °C was distinguishably lower than the emission for any other temperature. The optimum operating temperature for rubidium-argon-hydrogen over the range 470 °C - 650 °C was determined to be 535 °C. The data indicates that the catalysis reaction is sensitive to the cesium or rubidium vapor pressure with a decrease in rate due deviation from an optimum. At 10 watts input, cesium at 565 °C produced about 6 times the light output power of rubidium at any temperature. This indicates that the reaction is

much more dependent on the activity of the particular catalyst then on temperature within a reasonably broad temperature range.

In the cases where an anomalous optically measured power balance was observed, no possible chemical reactions of the tungsten filament cathode, the nickel mesh anode, the vaporized metal, and hydrogen or argon-hydrogen mixture gas at a cell temperature of about 650 °C could be found which accounted for the increased emission. In fact, no known chemical reaction releases enough energy to cause an anomalous plasma of hydrogen. Intense anomalous emission was observed for catalysts in the presence of hydrogen and no unusual behavior was observed for noncatalysts. This result indicates that the emission was due to a reaction of the catalyst with hydrogen. The catalyst enhancement of the emission was dramatically greater with an argon-hydrogen mixture versus pure hydrogen. This implies that the catalyst may increase the amount of Ar^+ catalyst to enhance the catalysis of hydrogen.

The most intense plasma was formed by a mixture of strontium and argon with hydrogen. The presence of a weak electric field may be necessary in order for strontium and Ar^+ to produce an anomalous discharge of hydrogen. In the case that electrons are ionized to a continuum energy level, the presence of a low strength electric field alters the continuum energy levels. The ionization energy of $188.2\,eV$ is 1% less than $m \cdot 27.2\,eV$ where $m = 7$, and the ionization energy of Ar^+ to Ar^{2+} is $27.6\,eV$. In the anomalous discharge of hydrogen due to the presence of strontium and Ar^+, the weak field may adjust the energy of ionizing strontium and Ar^+ to match the energy of $7 \cdot 27.2\,eV$ and $27.2\,eV$, respectively, to permit a novel reaction of atomic hydrogen.

The release of energy from hydrogen as evidenced by the anomalous emission must result in a lower-energy state of hydrogen. The theory is given in the Appendix. The lower-energy hydrogen atom called a hydrino atom by Mills [1] would be expected to demonstrate novel chemistry. Reports of the formation of novel compounds provide substantial evidence supporting a novel reaction of hydrogen as the mechanism of the observed anomalous discharge. Novel hydrogen compounds have been isolated as products of the reaction of atomic hydrogen with atoms and ions which formed an anomalous plasma in the present studies and previously reported in EUV studies [2-16]. Novel

inorganic alkali and alkaline earth hydrides of the formula MH^* and MH^*X wherein M is the metal, X, is a singly negatively charged anion, and H^* comprises a novel high binding energy hydride ion were synthesized in a high temperature gas cell by reaction of atomic hydrogen with a catalyst such as potassium metal and MH, MX or MX_2 corresponding to an alkali metal or alkaline earth metal compound, respectively [17, 20-21]. Novel hydride compounds were identified by 1.) time of flight secondary ion mass spectroscopy which showed a dominant hydride ion in the negative ion spectrum, 2.) X-ray photoelectron spectroscopy which showed novel hydride peaks and significant shifts of the core levels of the primary elements bound to the novel hydride ions, 3.) ^1H nuclear magnetic resonance spectroscopy (NMR) which showed extraordinary upfield chemical shifts compared to the NMR of the corresponding ordinary hydrides, and 4.) thermal decomposition with analysis by gas chromatography, and mass spectroscopy which identified the compounds as hydrides [17, 20].

The implications are that a new field of novel hydrogen chemistry has been discovered which may be a new power source that creates an energetic plasma. The plasma may be converted directly to electricity with high efficiency using a known microwave device called a gyrotron, thus, avoiding a heat engine such as a turbine. Plasma to electric conversion technology with no reformer, no fuel cost, creation of a valuable chemical by-product rather than pollutants such as carbon dioxide, and significantly lower capital costs and operating and maintenance (O&M) costs are anticipated to result in microdistributed units that are competitive with central power and significantly superior to competing microdistributed power technologies such as fuel cells [36].

APPENDIX

Mills [1] predicts that certain atoms or ions serve as catalysts to release energy from hydrogen to produce an increased binding energy hydrogen atom called a *hydrino atom* having a binding energy of

$$Binding\ Energy = \frac{13.6\ eV}{n^2} \tag{2}$$

where

$$n = \frac{1}{2}, \frac{1}{3}, \frac{1}{4}, \ldots, \frac{1}{p} \tag{3}$$

and p is an integer greater than 1, designated as $H\left[\frac{a_H}{p}\right]$ where a_H is the radius of the hydrogen atom. Hydrinos are predicted to form by reacting an ordinary hydrogen atom with a catalyst having a net enthalpy of reaction of about

$$m \cdot 27.2\ eV \tag{4}$$

where m is an integer. This catalysis releases energy from the hydrogen atom with a commensurate decrease in size of the hydrogen atom, $r_n = na_H$. For example, the catalysis of $H(n=1)$ to $H(n=1/2)$ releases $40.8\ eV$, and the hydrogen radius decreases from a_H to $\frac{1}{2}a_H$.

The excited energy states of atomic hydrogen are also given by Eq. (2) except that

$$n = 1, 2, 3, \ldots \tag{5}$$

The $n=1$ state is the "ground" state for "pure" photon transitions (the $n=1$ state can absorb a photon and go to an excited electronic state, but it cannot release a photon and go to a lower-energy electronic state). However, an electron transition from the ground state to a lower-energy state is possible by a nonradiative energy transfer such as multipole coupling or a resonant collision mechanism. These lower-energy states have fractional quantum numbers, $n = \frac{1}{\text{integer}}$. Processes that occur without photons and that require collisions are common. For example, the exothermic chemical reaction of $H + H$ to form H_2 does not occur with the emission of a photon. Rather, the reaction requires a collision with a third body, M, to remove the bond energy- $H + H + M \rightarrow H_2 + M^*$ [37]. The third body distributes the energy from the exothermic reaction, and the end result is the H_2 molecule and an increase in the temperature of the system. Some commercial phosphors are based on nonradiative energy transfer involving multipole coupling. For example, the strong absorption strength of Sb^{3+} ions along with the efficient nonradiative transfer of excitation from Sb^{3+} to Mn^{2+}, are responsible for the strong manganese luminescence from phosphors containing these ions [38]. Similarly, the $n=1$ state of hydrogen and the $n = \frac{1}{\text{integer}}$ states of hydrogen are

nonradiative, but a transition between two nonradiative states is possible via a nonradiative energy transfer, say $n=1$ to $n=1/2$. In these cases, during the transition the electron couples to another electron transition, electron transfer reaction, or inelastic scattering reaction which can absorb the exact amount of energy that must be removed from the hydrogen atom. Thus, a catalyst provides a net positive enthalpy of reaction of $m \cdot 27.2\ eV$ (i.e. it absorbs $m \cdot 27.2\ eV$ where m is an integer). Certain atoms or ions serve as catalysts which resonantly accept energy from hydrogen atoms and release the energy to the surroundings to effect electronic transitions to fractional quantum energy levels.

Catalysts

The emission must have been due to a novel chemical reaction between catalyst and atomic hydrogen. According to Mills [1], a catalytic system is provided by the ionization of t electrons from an atom or ion to a continuum energy level such that the sum of the ionization energies of the t electrons is approximately $m\,X\,27.2\ eV$ where m is an integer.

Potassium Metal

One such atomic catalytic system involves potassium metal. The first, second, and third ionization energies of potassium are $4.34066\ eV$, $31.63\ eV$, $45.806\ eV$, respectively [32]. The triple ionization ($t=3$) reaction of K to K^{3+}, then, has a net enthalpy of reaction of $81.7766\ eV$, which is equivalent to $m=3$ in Eq. (4).

$$81.7766\ eV + K(m) + H\left[\frac{a_H}{p}\right] \rightarrow K^{3+} + 3e^- + H\left[\frac{a_H}{(p+3)}\right] + [(p+3)^2 - p^2]X13.6\ eV \qquad (6)$$

$$K^{3+} + 3e^- \rightarrow K(m) + 81.7766\ eV \qquad (7)$$

And, the overall reaction is

$$H\left[\frac{a_H}{p}\right] \rightarrow H\left[\frac{a_H}{(p+3)}\right] + [(p+3)^2 - p^2]X13.6\ eV \qquad (8)$$

Rubidium Ion

Rubidium ions formed in the glow discharge can also provide a net enthalpy of a multiple of that of the potential energy of the hydrogen

atom. The second ionization energy of rubidium is $27.28\,eV$. The reaction Rb^{+} to Rb^{2+} has a net enthalpy of reaction of $27.28\,eV$, which is equivalent to $m=1$ in Eq. (4).

$$27.28\,eV + Rb^{+} + H\left[\frac{a_H}{p}\right] \rightarrow Rb^{2+} + e^{-} + H\left[\frac{a_H}{(p+1)}\right] + [(p+1)^2 - p^2]X13.6\,eV \tag{9}$$

$$Rb^{2+} + e^{-} \rightarrow Rb^{+} + 27.28\,eV \tag{10}$$

The overall reaction is

$$H\left[\frac{a_H}{p}\right] \rightarrow H\left[\frac{a_H}{(p+1)}\right] + [(p+1)^2 - p^2]\,X\,13.6\,eV \tag{11}$$

Cesium Metal

A catalytic system is provided by the ionization of 2 electrons from a cesium atom each to a continuum energy level such that the sum of the ionization energies of the 2 electrons is approximately $27.2\,eV$. The first and second ionization energies of cesium are $3.89390\,eV$ and $23.15745\,eV$, respectively [32]. The double ionization reaction of Cs to Cs^{2+}, then, has a net enthalpy of reaction of $27.05135\,eV$, which is equivalent to $m=1$ in Eq. (4).

$$27.05135\,eV + Cs(m) + H\left[\frac{a_H}{p}\right] \rightarrow Cs^{2+} + 2e^{-} + H\left[\frac{a_H}{(p+1)}\right] + [(p+1)^2 - p^2]X13.6\,eV \tag{12}$$

$$Cs^{2+} + 2e^{-} \rightarrow Cs(m) + 27.05135\,eV \tag{13}$$

And, the overall reaction is

$$H\left[\frac{a_H}{p}\right] \rightarrow H\left[\frac{a_H}{(p+1)}\right] + [(p+1)^2 - p^2]X13.6\,eV \tag{14}$$

Strontium Metal

Another catalytic system involves strontium. The first through the fifth ionization energies of strontium are $5.69484\,eV$, $11.03013\,eV$, $42.89\,eV$, $57\,eV$, and $71.6\,eV$, respectively [32]. The ionization reaction of Sr to Sr^{5+}, $(t=5)$, then, has a net enthalpy of reaction of $188.2\,eV$, which is equivalent to $m=7$ in Eq. (4).

$$188.2\ eV + Sr(m) + H\left[\frac{a_H}{p}\right] \rightarrow Sr^{5+} + 5e^- + H\left[\frac{a_H}{(p+7)}\right] + [(p+7)^2 - p^2]X13.6\ eV \quad (15)$$

$$Sr^{5+} + 5e^- \rightarrow Sr(m) + 188.2\ eV \quad (16)$$

And, the overall reaction is

$$H\left[\frac{a_H}{p}\right] \rightarrow H\left[\frac{a_H}{(p+7)}\right] + [(p+7)^2 - p^2]X13.6\ eV \quad (17)$$

Argon Ion

Argon ions can also provide a net enthalpy of a multiple of that of the potential energy of the hydrogen atom. The second ionization energy of argon is $27.63\ eV$. The reaction Ar^+ to Ar^{2+} has a net enthalpy of reaction of $27.63\ eV$, which is equivalent to $m=1$ in Eq. (4).

$$27.63\ eV + Ar^+ + H\left[\frac{a_H}{p}\right] \rightarrow Ar^{2+} + e^- + H\left[\frac{a_H}{(p+1)}\right] + [(p+1)^2 - p^2]X13.6\ eV \quad (18)$$

$$Ar^{2+} + e^- \rightarrow Ar^+ + 27.63\ eV \quad (19)$$

And, the overall reaction is

$$H\left[\frac{a_H}{p}\right] \rightarrow H\left[\frac{a_H}{(p+1)}\right] + [(p+1)^2 - p^2]X13.6\ eV \quad (20)$$

Hydride Ion

A novel hydride ion having extraordinary chemical properties given by Mills [1] is predicted to form by the reaction of an electron with a hydrino (Eq. (21)). The resulting hydride ion is referred to as a hydrino hydride ion, designated as $H^-(1/p)$.

$$H\left[\frac{a_H}{p}\right] + e^- \rightarrow H^-(1/p) \quad (21)$$

The hydrino hydride ion is distinguished from an ordinary hydride ion having a binding energy of 0.8 eV. The hydrino hydride ion is predicted [1] to comprise a hydrogen nucleus and two indistinguishable electrons at a binding energy according to the following formula:

$$Binding\ Energy = \frac{\hbar^2\sqrt{s(s+1)}}{8\mu_e a_0^2\left[\frac{1+\sqrt{s(s+1)}}{p}\right]^2} - \frac{\pi\mu_0 e^2\hbar^2}{m_e^2 a_0^3}\left(1+\frac{2^2}{\left[\frac{1+\sqrt{s(s+1)}}{p}\right]^3}\right) \quad (22)$$

where p is an integer greater than one, $s=1/2$, π is pi, $\hbar$ is Planck's constant bar, μ_o is the permeability of vacuum, m_e is the mass of the electron, μ_e is the reduced electron mass, a_o is the Bohr radius, and e is the elementary charge. The ionic radius is

$$r_1 = \frac{a_0}{p}\left(1+\sqrt{s(s+1)}\right);\ s=\frac{1}{2} \quad (23)$$

From Eq. (23), the radius of the hydrino hydride ion $H^-(1/p);\ p = \text{integer}$ is $\frac{1}{p}$ that of ordinary hydride ion, $H^-(1/1)$. Compounds containing hydrino hydride ions have been isolated as products of the reaction of atomic hydrogen with atoms and ions identified as catalysts by EUV emission [2-31].

ACKNOWLEDGMENT

Special thanks to Mark Nanstell for developing some of the glow discharge and visible spectroscopy methods and to Bala Dhandapani for logistics and for reviewing this manuscript.

REFERENCES

1. R. Mills, The Grand Unified Theory of Classical Quantum Mechanics, January 2000 Edition, BlackLight Power, Inc., Cranbury, New Jersey, Distributed by Amazon.com.
2. R. Mills, "Spectroscopic Identification of a Novel Catalytic Reaction of Atomic Hydrogen and the Hydride Ion Product", Int. J. Hydrogen Energy, submitted.
3. R. Mills and M. Nansteel, "Anomalous Argon-Hydrogen-Strontium

Discharge", IEEE Transactions of Plasma Science, submitted.
4. R. Mills, M. Nansteel, and Y. Lu, "Anomalous Hydrogen-Strontium Discharge", European Journal of Physics D, submitted.
5. R. Mills, J. Dong, Y. Lu, "Observation of Extreme Ultraviolet Hydrogen Emission from Incandescently Heated Hydrogen Gas with Certain Catalysts", Int. J. Hydrogen Energy, Vol. 25, (2000), pp. 919-943.
6. R. Mills, "Observation of Extreme Ultraviolet Emission from Hydrogen-KI Plasmas Produced by a Hollow Cathode Discharge", Int. J. Hydrogen Energy, in press.
7. R. Mills, "Temporal Behavior of Light-Emission in the Visible Spectral Range from a Ti-K2CO3-H-Cell", Int. J. Hydrogen Energy, in press.
8. R. Mills, Y. Lu, and T. Onuma, "Formation of a Hydrogen Plasma from an Incandescently Heated Hydrogen-Catalyst Gas Mixture with an Anomalous Afterglow Duration", Int. J. Hydrogen Energy, in press.
9. R. Mills, M. Nansteel, and Y. Lu, "Observation of Extreme Ultraviolet Hydrogen Emission from Incandescently Heated Hydrogen Gas with Strontium that Produced an Anomalous Optically Measured Power Balance", Int. J. Hydrogen Energy, in press.
10. R. Mills, J. Dong, Y. Lu, J. Conrads, "Observation of Extreme Ultraviolet Hydrogen Emission from Incandescently Heated Hydrogen Gas with Certain Catalysts", 1999 Pacific Conference on Chemistry and Spectroscopy and the 35th ACS Western Regional Meeting, Ontario Convention Center, California, (October 6-8, 1999).
11. R. Mills, J. Dong, N. Greenig, and Y. Lu, "Observation of Extreme Ultraviolet Hydrogen Emission from Incandescently Heated Hydrogen Gas with Certain Catalysts", National Hydrogen Association, 11 th Annual U.S. Hydrogen Meeting, Vienna, VA, (February 29-March 2, 2000).
12. R. Mills, B. Dhandapani, N. Greenig, J. He, J. Dong, Y. Lu, and H. Conrads, "Formation of an Energetic Plasma and Novel Hydrides from Incandescently Heated Hydrogen Gas with Certain Catalysts", National Hydrogen Association, 11 th Annual U.S. Hydrogen Meeting, Vienna, VA, (February 29-March 2, 2000).
13. Mills, J. Dong, N. Greenig, and Y. Lu, "Observation of Extreme Ultraviolet Hydrogen Emission from Incandescently Heated Hydrogen Gas with Certain Catalysts", 219 th National ACS Meeting, San

Francisco, California, (March 26-30, 2000).
14. R. Mills, B. Dhandapani, N. Greenig, J. He, J. Dong, Y. Lu, and H. Conrads, "Formation of an Energetic Plasma and Novel Hydrides from Incandescently Heated Hydrogen Gas with Certain Catalysts", 219 th National ACS Meeting, San Francisco, California, (March 26-30, 2000).
15. R. Mills, B. Dhandapani, N. Greenig, J. He, J. Dong, Y. Lu, and H. Conrads, "Formation of an Energetic Plasma and Novel Hydrides from Incandescently Heated Hydrogen Gas with Certain Catalysts", June ACS Meeting (29th Northeast Regional Meeting, University of Connecticut, Storrs, CT, (June 18-21, 2000)).
16. R. Mills, B. Dhandapani, N. Greenig, J. He, J. Dong, Y. Lu, and H. Conrads, "Formation of an Energetic Plasma and Novel Hydrides from Incandescently Heated Hydrogen Gas with Certain Catalysts", August National ACS Meeting (220th ACS National Meeting, Washington, DC, (August 20-24, 2000)).
17. R. Mills, B. Dhandapani, N. Greenig, J. He, "Synthesis and Characterization of Potassium Iodo Hydride", Int. J. of Hydrogen Energy, Vol. 25, Issue 12, December, (2000), pp. 1185-1203.
18. R. Mills, "Novel Inorganic Hydride", Int. J. of Hydrogen Energy, Vol. 25, (2000), pp. 669-683.
19. R. Mills, "Novel Hydrogen Compounds from a Potassium Carbonate Electrolytic Cell", Fusion Technology, Vol. 37, No. 2, March, (2000), pp. 157-182.
20. R. Mills, B. Dhandapani, M. Nansteel, J. He, T. Shannon, A. Echezuria, "Synthesis and Characterization of Novel Hydride Compounds", Int. J. of Hydrogen Energy, in press.
21. R. Mills, B. Dhandapani, M. Nansteel, J. He, A. Voigt, Identification of Compounds Containing Novel Hydride Ions by Nuclear Magnetic Resonance Spectroscopy, Int. J. Hydrogen Energy, submitted.
22. R. Mills, "Highly Stable Novel Inorganic Hydrides", Journal of Materials Research, submitted.
23. R. Mills, "Novel Hydride Compound", 1999 Pacific Conference on Chemistry and Spectroscopy and the 35th ACS Western Regional Meeting, Ontario Convention Center, California, (October 6-8, 1999).
24. R. Mills, B, Dhandapani, N. Greenig, J. He, "Synthesis and Characterization of Potassium Iodo Hydride", 1999 Pacific Conference

on Chemistry and Spectroscopy and the 35th ACS Western Regional Meeting, Ontario Convention Center, California, (October 6-8, 1999).
25. R. Mills, J. He, and B. Dhandapani, "Novel Hydrogen Compounds", 1999 Pacific Conference on Chemistry and Spectroscopy and the 35th ACS Western Regional Meeting, Ontario Convention Center, California, (October 6-8, 1999).
26. R. Mills, "Novel Hydride Compound", National Hydrogen Association, 11 th Annual U.S. Hydrogen Meeting, Vienna, VA, (February 29-March 2, 2000).
27. R. Mills, J. He, and B. Dhandapani, "Novel Alkali and Alkaline Earth Hydrides", National Hydrogen Association, 11 th Annual U.S. Hydrogen Meeting, Vienna, VA, (February 29-March 2, 2000).
28. R. Mills, "Novel Hydride Compound", 219 th National ACS Meeting, San Francisco, California, (March 26-30, 2000).
29. R. Mills, J. He, and B. Dhandapani, "Novel Alkali and Alkaline Earth Hydrides", 219 th National ACS Meeting, San Francisco, California, (March 26-30, 2000).
30. R. Mills, J. He, and B. Dhandapani, "Novel Alkali and Alkaline Earth Hydrides", August National ACS Meeting (220 th ACS National Meeting, Washington, DC, (August 20-24, 2000)).
31. R. Mills, W. Good, A. Voigt, Jinquan Dong, "Minimum Heat of Formation of Potassium Iodo Hydride", Int. J. Hydrogen Energy, submitted.
32. David R. Linde, *CRC Handbook of Chemistry and Physics*, 79 th Edition, CRC Press, Boca Raton, Florida, (1998-9), p. 10-175 to p. 10-177.
33. R. Mills, The Nature of Free Electrons in Superfluid Helium--a Test of Quantum Mechanics and a Basis to Review its Foundations and Make a Comparison to Classical Theory, Int. J. Hydrogen Energy, in press.
34. R. Mills, "The Hydrogen Atom Revisited", Int. J. of Hydrogen Energy, Vol. 25, Issue 12, December, (2000), pp. 1171-1183.
35. C. L. Yaws, *Chemical Properties Handbook*, McGraw-Hill, (1999).
36. R. Mills, "BlackLight Power Technology-A New Clean Energy Source with the Potential for Direct Conversion to Electricity", Global Foundation, Inc. conference entitled *Global Warming and Energy Policy*, Fort Lauderdale, FL, November 26-28, 2000.
37. N. V. Sidgwick, *The Chemical Elements and Their Compounds*, Volume I, Oxford, Clarendon Press, (1950), p.17.

38. M. D. Lamb, *Luminescence Spectroscopy*, Academic Press, London, (1978), p. 68.

TABLE 1. Vapor pressure of metals versus temperature.

T (°C)	Na P_v (Torr)[a]	K P_v (Torr)[a]	Rb P_v (Torr)[a]	Cs P_v (Torr)[a]	Mg P_v (Torr)[a]	Sr P_v (Torr)[a]
470	2.0	16.7	43.2	65.9	0.030	0.001
500	3.8	28.3	68.9	101.5	0.075	0.004
520	5.6	39.3	92.1	132.6	0.132	0.007
535	7.5	49.8	113.4	160.5	0.197	0.011
540	8.3	53.8	121.3	170.8	0.225	0.012
560	12.0	72.4	157.7	217.0	0.372	0.022
600	23.6	125.8	256.8	337.7	0.947	0.061
620	32.4	162.8	322.2	414.4	1.459	0.100
650	50.9	234.4	444.5	552.9	2.682	0.197

[a] Calculated [35]

Figure Captions

Figure 1. The electrode assembly of the glow discharge cell.

Figure 2. The stainless steel cell and experimental setup for generating a glow discharge plasma and optically measuring the power balance from 1.) hydrogen, argon, argon-hydrogen mixture (97/3%), and argon-hydrogen mixture (90/10%), 2.) sodium, magnesium, cesium, potassium, rubidium, and strontium with hydrogen, 3.) sodium, magnesium, cesium, potassium, rubidium, and strontium with argon, 4.) sodium, magnesium, cesium, potassium, rubidium, and strontium with argon-hydrogen mixture (97/3%), and 5.) potassium with argon-hydrogen mixture (90/10%).

Figure 3. The comparison of the light output power ($\mu W/cm^2$) of H_2 alone —▲—, Ar alone —△—, Ar + H_2 (97/3%) —×—, Ar + H_2 (90/10%) —■—, Na + H_2 —▲—, Mg + H_2 —▲—, K + H_2 —◆—, Na + Ar —△—, Mg + Ar —△—, K + Ar —△—, Rb + Ar —△—, Cs + Ar —△—, Sr + Ar —△—, Na + Ar + H_2 (97/3%) —×—, Mg + Ar + H_2 (97/3%) —×—, K + Ar + H_2 (97/3%) —✱—, Rb + Ar + H_2 (97/3%) —+—, Cs + Ar + H_2 (97/3%) —·—, Sr + Ar + H_2 (97/3%) —◇—, and K + Ar + H_2 (90/10%) —□— showing the 0-50 $\mu W/cm^2$ range with Cs + Ar + H_2 (97/3%) —·— and Sr + Ar + H_2 (97/3%) —◇— off-scale.

Figure 4. The comparison of the light output power ($\mu W/cm^2$) of H_2 alone —▲—, Ar alone —△—, Ar + H_2 (97/3%) —×—, Ar + H_2 (90/10%) —■—, Na + H_2 —▲—, Mg + H_2 —▲—, K + H_2 —◆—, Na + Ar —△—, Mg + Ar —△—, K + Ar —△—, Rb + Ar —△—, Cs + Ar —△—, Sr + Ar —△—, Na + Ar + H_2 (97/3%) —×—, Mg + Ar + H_2 (97/3%) —×—, K + Ar + H_2 (97/3%) —✱—, Rb + Ar + H_2 (97/3%) —+—, Cs + Ar + H_2 (97/3%) —·—, Sr + Ar + H_2 (97/3%) —◇—, and K + Ar + H_2 (90/10%) —□— showing the 0-200 $\mu W/cm^2$ range with Sr + Ar + H_2 (97/3%) —◇— off-scale.

Figure 5. The comparison of the light output power ($\mu W/cm^2$) of H_2 alone —▲—, Ar alone —△—, Ar + H_2 (97/3%) —×—, Ar + H_2 (90/10%) —■—, Na + H_2 —▲—, Mg + H_2 —▲—, K + H_2 —◆—, Na + Ar —△—, Mg + Ar —△—, K + Ar —△—, Rb + Ar —△—, Cs + Ar —△—, Sr + Ar —△—, Na + Ar + H_2 (97/3%) —×—, Mg + Ar + H_2 (97/3%) —×—, K + Ar + H_2 (97/3%) —✱—, Rb + Ar + H_2 (97/3%) —+—, Cs + Ar + H_2 (97/3%) —·—, Sr + Ar + H_2 (97/3%) —◇—, and K + Ar + H_2 (90/10%) —□— showing the 0-800 $\mu W/cm^2$

range.

Figure 6. The comparison of the light output power ($\mu W/cm^2$) of K + Ar + H_2 (97/3%) at a cell temperature of 650 °C —+—, Rb + Ar + H_2 (97/3%) at a cell temperature of 650 °C —•—, Cs + Ar + H_2 (97/3%) at a cell temperature of 480 °C —✱—, Cs + Ar + H_2 (97/3%) at a cell temperature of 500 °C —■—, Cs + Ar + H_2 (97/3%) at a cell temperature of 520 °C —▲—, Cs + Ar + H_2 (97/3%) at a cell temperature of 540 °C —×—, Cs + Ar + H_2 (97/3%) at a cell temperature of 565 °C —◆—, and Cs + Ar + H_2 (97/3%) at a cell temperature of 600 °C —□—.

Figure 7. The comparison of the light output power ($\mu W/cm^2$) of Cs + Ar + H_2 (97/3%) at a cell temperature of 565 °C —•—, Rb + Ar + H_2 (97/3%) at a cell temperature of 470 °C —◆—, Rb + Ar + H_2 (97/3%) at a cell temperature of 500 °C —■—, Rb + Ar + H_2 (97/3%) at a cell temperature of 535 °C —▲—, Rb + Ar + H_2 (97/3%) at a cell temperature of 560 °C —×—, Rb + Ar + H_2 (97/3%) at a cell temperature of 600 °C —✱—, Rb + Ar + H_2 (97/3%) at a cell temperature of 620 °C —◇—, and Rb + Ar + H_2 (97/3%) at a cell temperature of 650 °C —+—.

FIGURE 1.

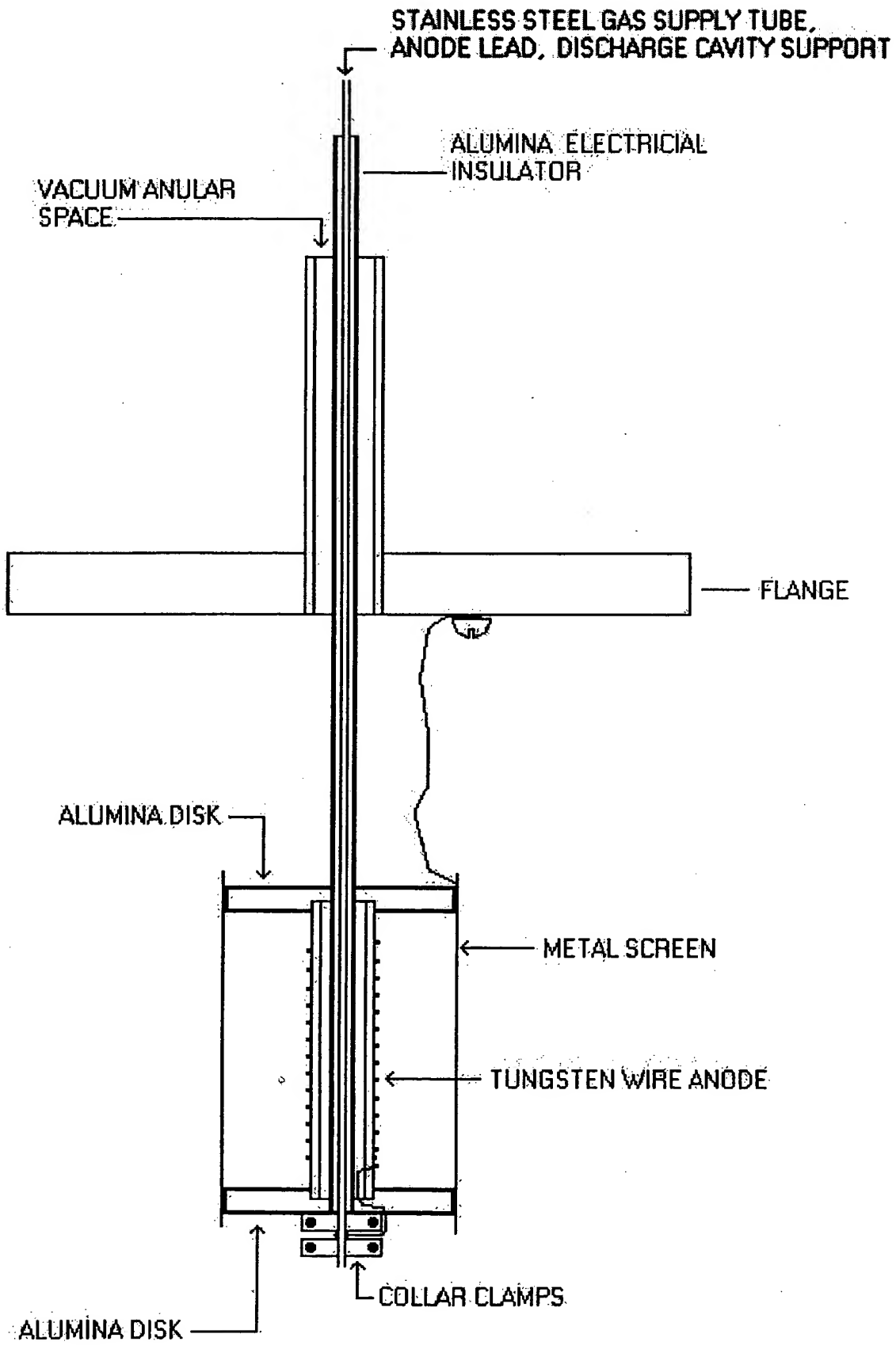
STAINLESS STEEL GAS SUPPLY TUBE,
ANODE LEAD, DISCHARGE CAVITY SUPPORT
ALUMINA ELECTRICIAL
INSULATOR
VACUUM ANULAR
SPACE
FLANGE
ALUMINA DISK
METAL SCREEN
TUNGSTEN WIRE ANODE
COLLAR CLAMPS
ALUMINA DISK

FIGURE 2.

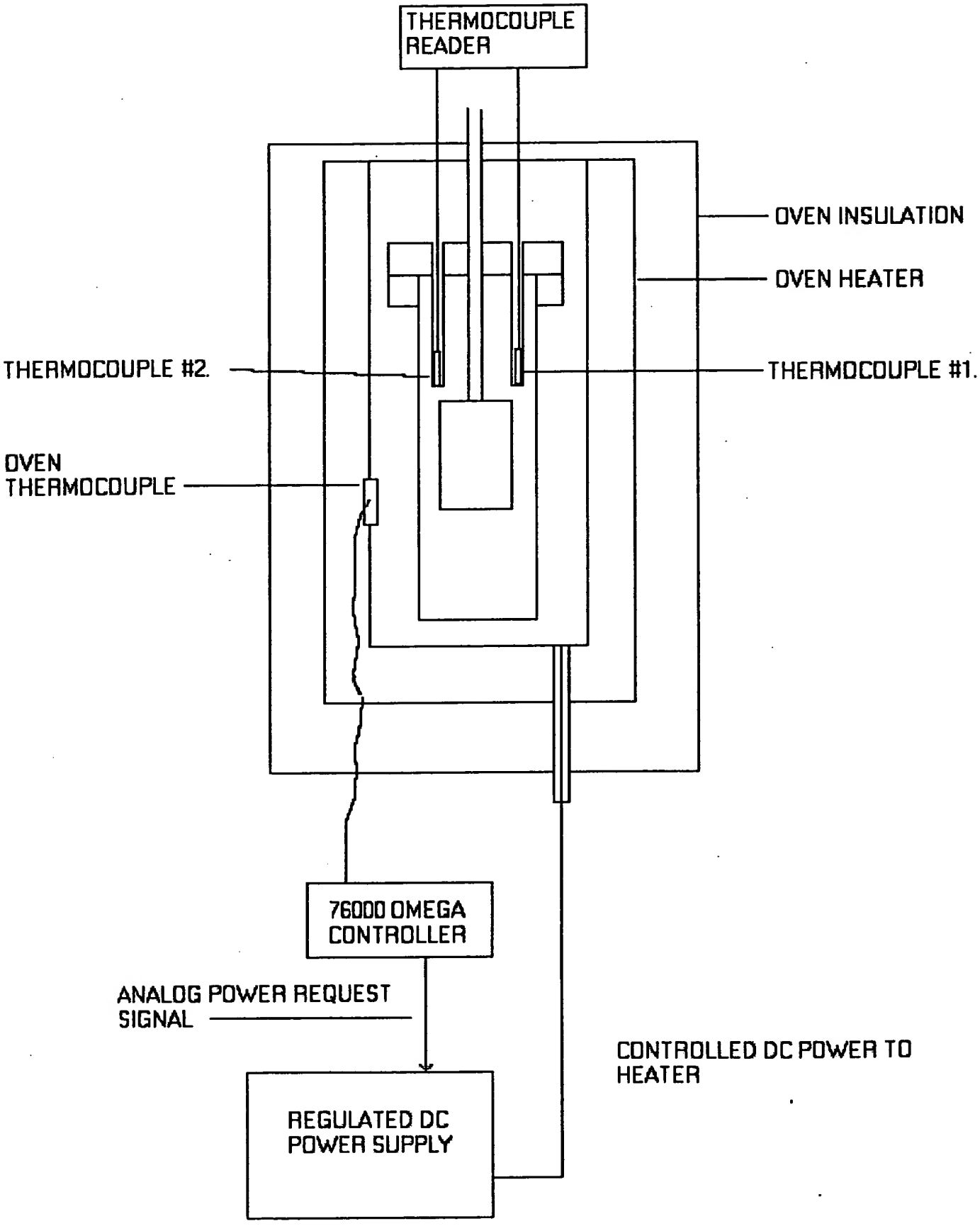
THERMOCOUPLE READER
OVEN INSULATION
OVEN HEATER
THERMOCOUPLE #2.
THERMOCOUPLE #1.
OVEN THERMOCOUPLE
76000 OMEGA CONTROLLER
ANALOG POWER REQUEST SIGNAL
CONTROLLED DC POWER TO HEATER
REGULATED DC POWER SUPPLY

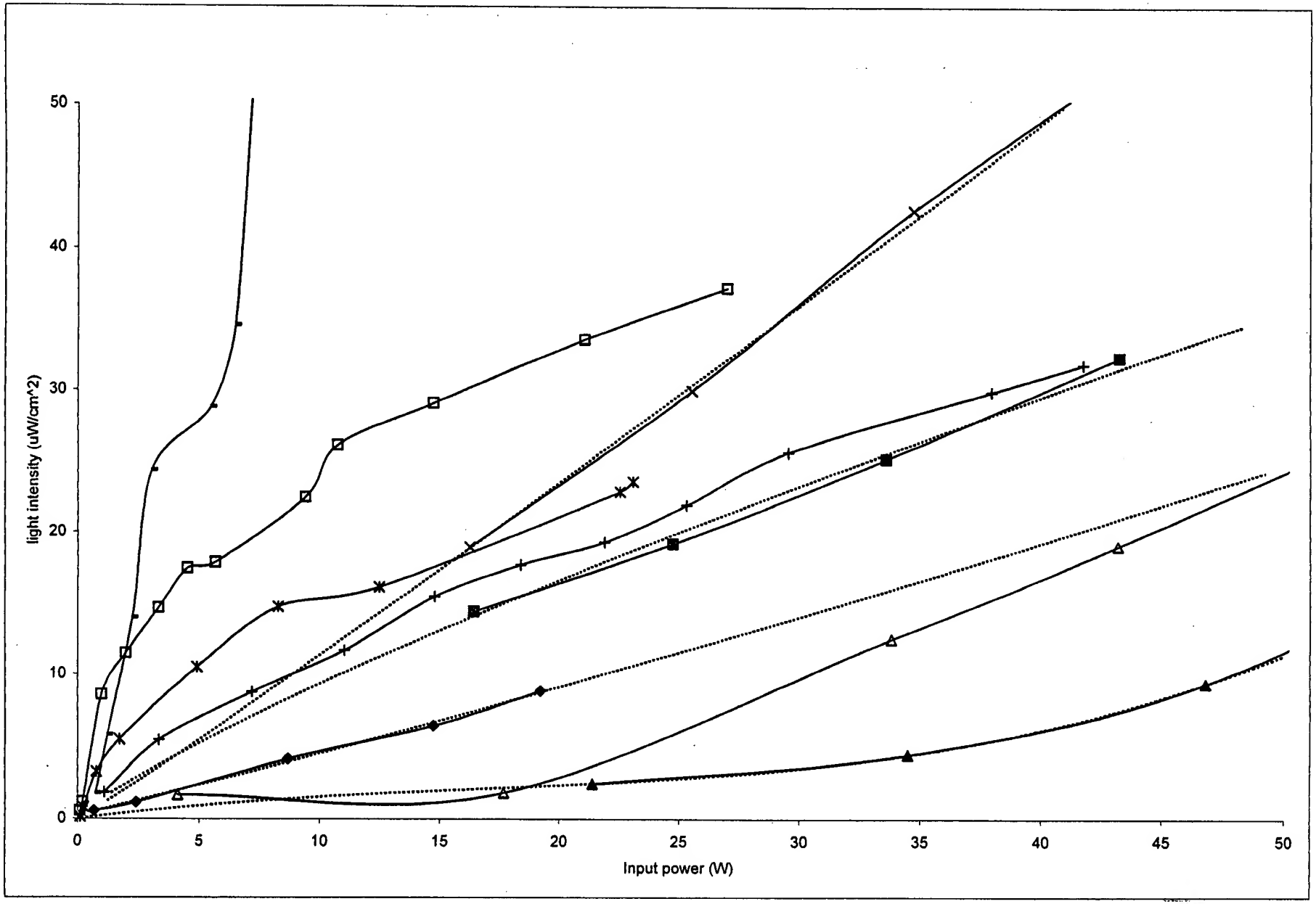
light intensity (uW/cm^2)
Input power (W)
0
10
20
30
40
50
0
5
10
15
20
25
30
35
40
45
50

Fig. 3

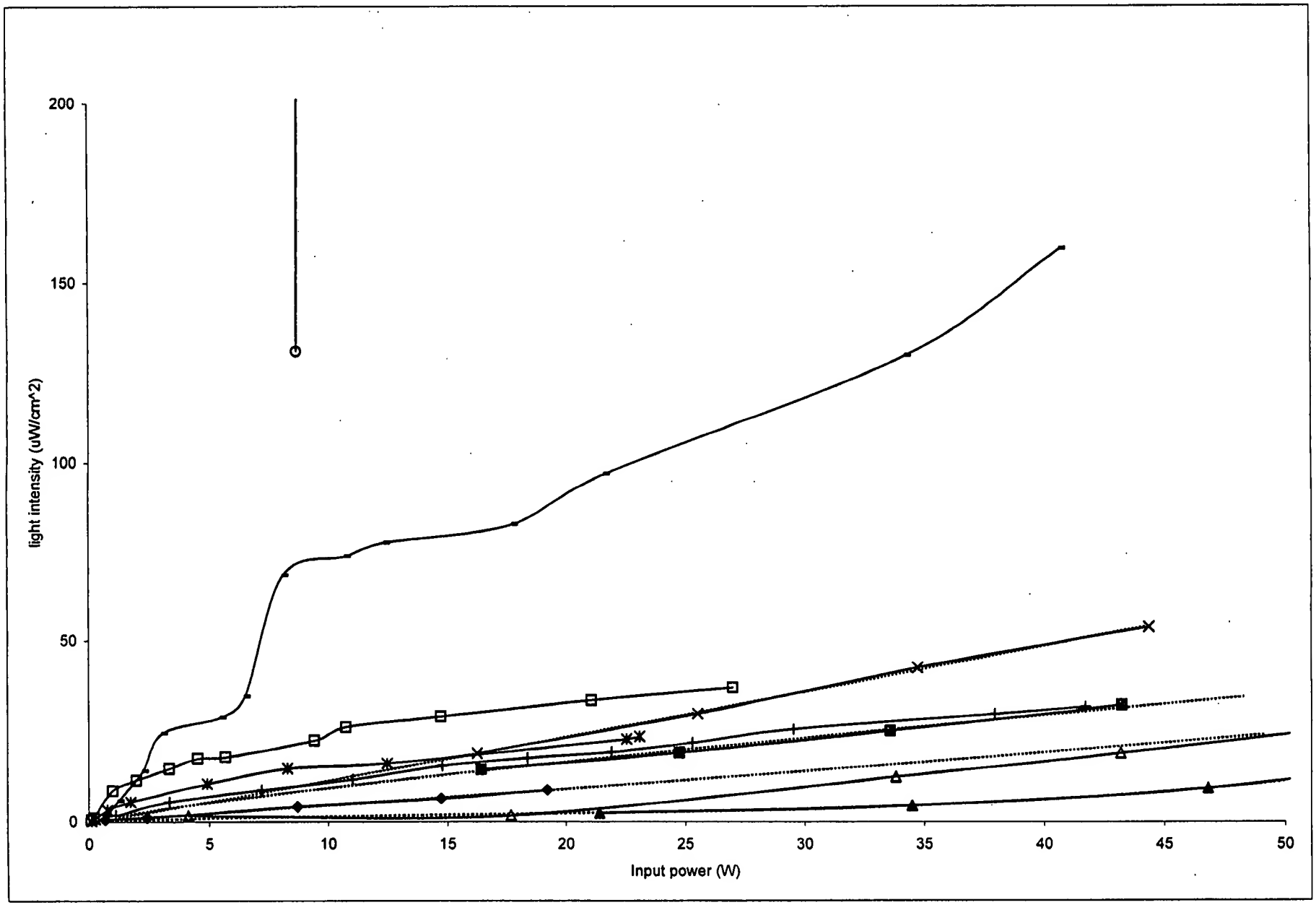
200
150
100
50
0
light intensity (uW/cm^2)
0
5
10
15
20
25
30
35
40
45
50
Input power (W)

Fig. 4

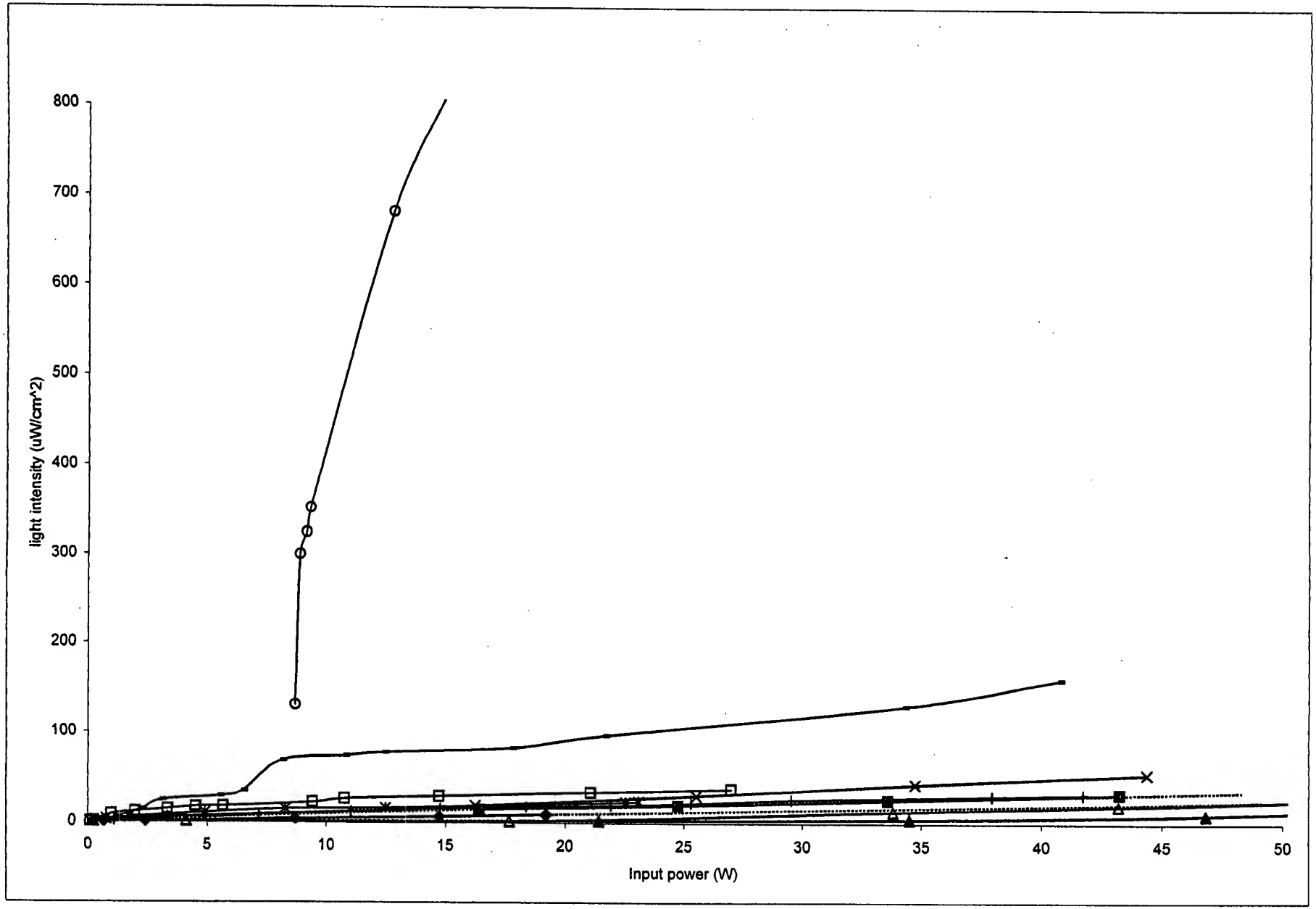
800
700
600
500
400
300
200
100
0
light intensity (uW/cm^2)
0
5
10
15
20
25
30
35
40
45
50
Input power (W)

Fig. 5

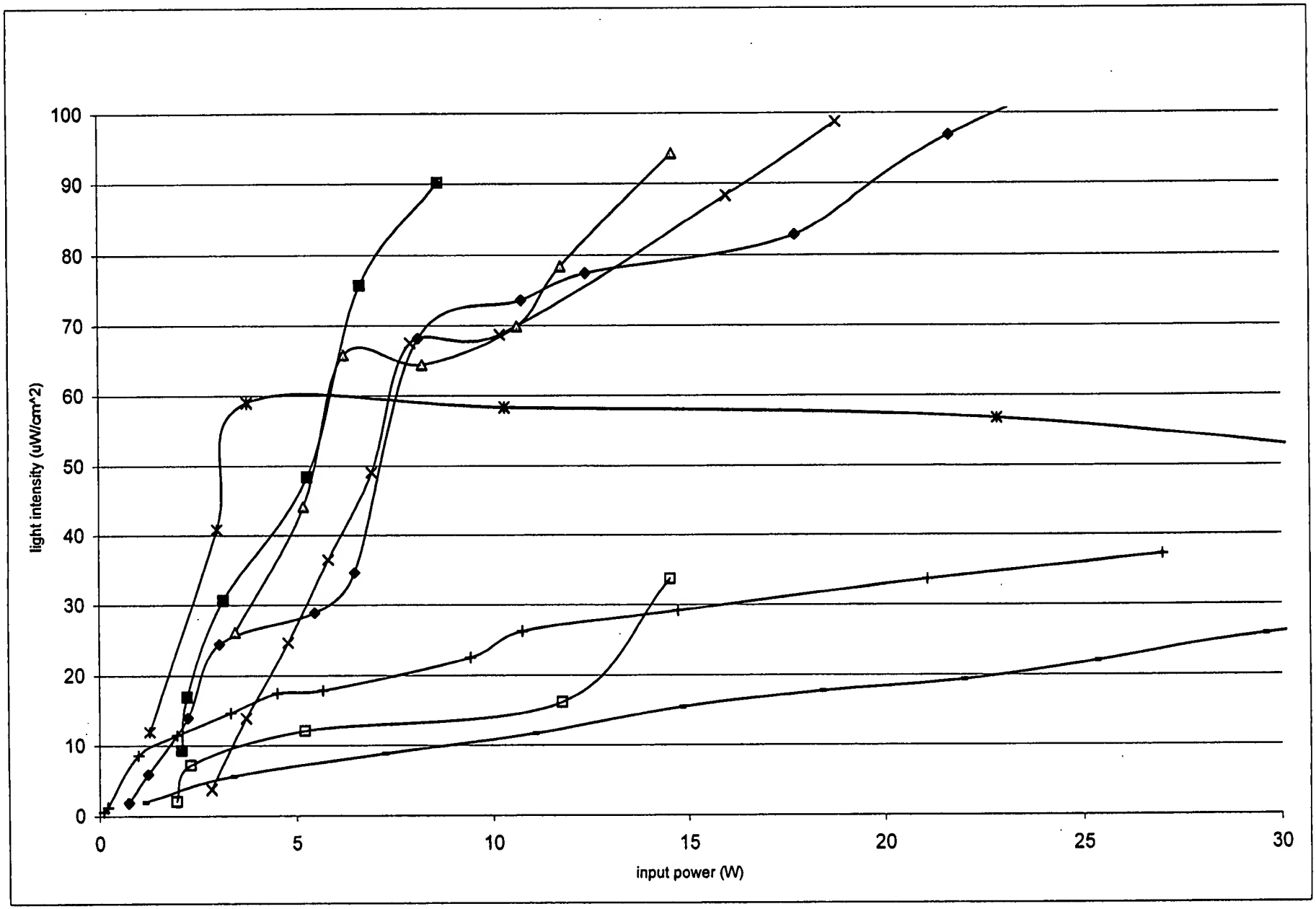
light intensity (uW/cm^2)
input power (W)
0
10
20
30
40
50
60
70
80
90
100
0
5
10
15
20
25
30

Fig. 6

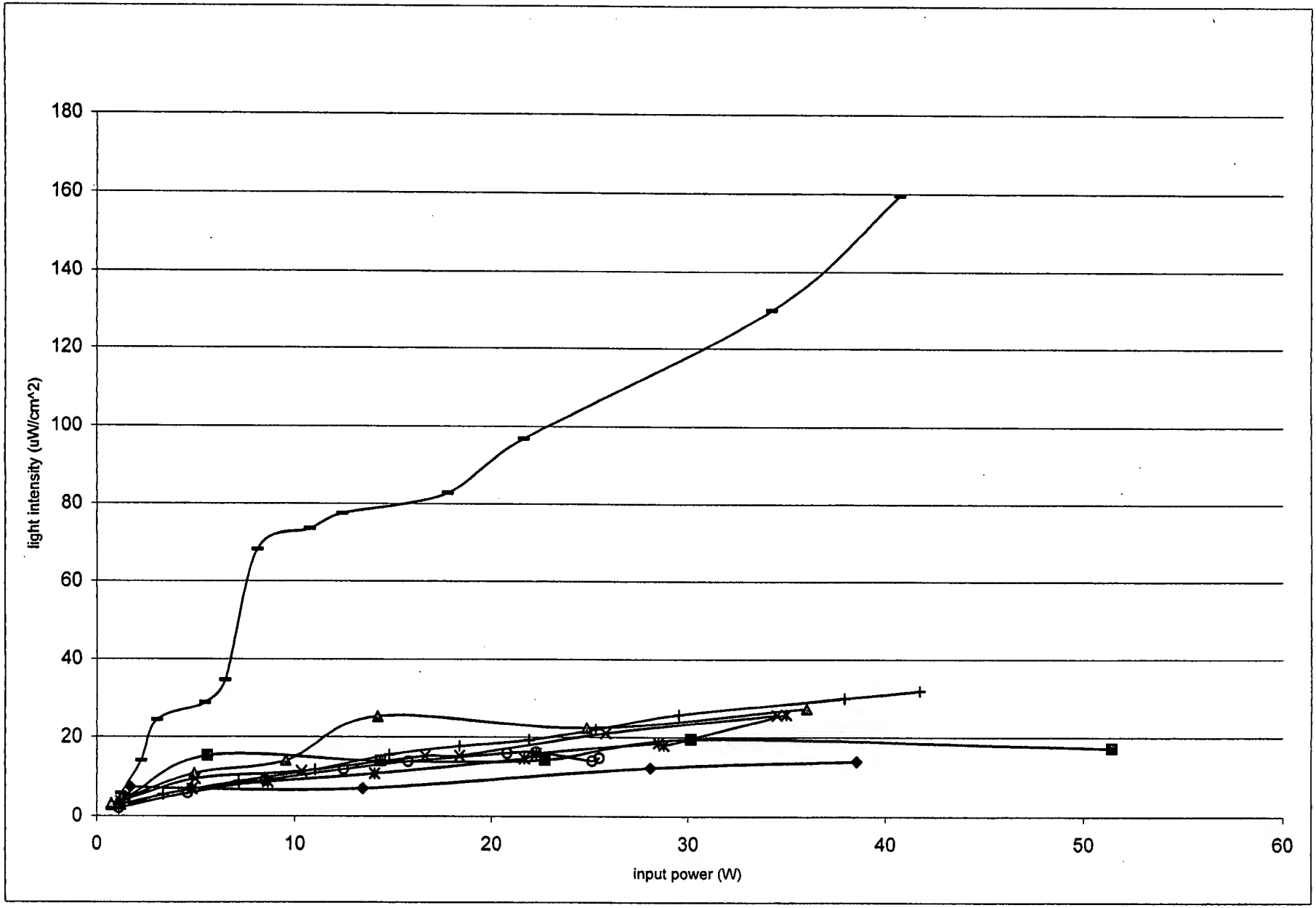
180
160
140
120
100
80
60
40
20
0
light intensity (uW/cm^2)
0
10
20
30
40
50
60
input power (W)

Fig. 7